

Light Weight CNN Model for Accurate and Efficient Skin Cancer Classification

1stC.Rohith Bhat
Department of CSE

Saveetha School of Engineering, Saveetha
University, Chennai, India.
rohithbhat2000@gmail.com

2ndK.Kodeeswari,
Department of ECE

Kongu Engineering college, Erode,India.
kodees26@gmail.com

3rdP.Narmatha,
Department of ECE

Sairam college of Engineering, Bangalore,
India.
narmathaphd@gmail.com

4thM R Archana Jenis
Department of CSE

St.Joseph's college of Engineering,
Chennai, India.
archana10906@gmail.com

5th Harishchander Anandaram,

Amrita school of Artificial Intelligence,
Amrita Vishwa Vidyapeetham, Coimbatore,
Tamilnadu,India.

[a harishchander@cb.amrita.edu](mailto:harishchander@cb.amrita.edu)

6thD.Narayani,

Department of Computer applications,
School of computing sciences, Vels institute
of science technology and advanced
studies, Chennai, India.
narayanivistas@gmail.com

Abstract-This paper, proposes a lightweight model: a modified Convolutional Neural Network (CNN) to perform the multi-class skin cancer classification with the HAM10000 dermoscopic image dataset. The architecture of the proposed model is capable of detecting seven skin lesion categories through computationally efficient operations including: separable convolutions, Swish activation, spatial dropout, and global average pooling. These architectural improvements significantly speed up the model convergence and legitimate the number of parameters but it still performs on high scale. The data is pre-processed using median filter, standardization, and augmentation to handle the class imbalances. Experiments show that by training in 220 seconds, DCN can achieve 95% accuracy, surpassing several popular benchmarks of deep learning such as InceptionV4 and ResNet50 in terms of both time and space efficiency. This renders the model to be very applicable for real-time diagnosis at healthcare facilities with mobile or limited resources.

Keywords: Skin Cancer Classification, Lightweight CNN, HAM10000, Separable Convolution, Medical Image Analysis.

I INTRODUCTION

Skin cancer is one of the most prevalent cancers globally, and early detection is crucial for the improvement of survival rates and decreasing healthcare cost. Conventional diagnosis such as clinical examination and histopathology is subjected to subjective interpretation and requires expert to interpret, limiting the ability to use for large-scale screening [1]. In the last years, deep learning methods such as Convolutional Neural Networks (CNNs) have been highly successful in medical image analysis and they have demonstrated to be an effective tool for the automatic classification of skin lesions [2], [3].

However, modern CNN models, such as InceptionV4, ResNet50, EfficientNet, are resource hungry and require significant computation resources thus rendering them not real-time for diagnosis on mobile or edge devices [4]. Such models will usually need high-level GPUs, long training time and large memory consumption, which is not practical in low-resource clinical applications. To address these limitations, lightweight CNN models have been proposed with lower complexity but comparable performance [5], [6].

In this study, we propose a simple lightweight CNN model for the multi-class classification of skin lesion by using HAM10000 dataset. The proposed model

can differentiate 7 types of skin lesions such as Nevus, Melanoma, Basal Cell Carcinoma, Actinic Keratosis, Seborrheic Keratosis, Vascular Lesions, and Dermatofibroma successfully with high accuracy and low computational cost [7]. The architecture relies on the state-of-the-art deep learning methods, including Swish activation functions, Spatial Dropout, Separable Convolutions, and Global Average Pooling, as a means to enhance generalization, prevent overfitting, and speed-up the training process [8], [9].

Recent models like TurkerNet and EFAM-Net have shown good performances utilizing efficient CNN blocks and attention layers to deal with class imbalance and overfitting problems in skin cancer datasets [5], [10]. Hybrid models based on metaheuristic optimization and deep learning have further enhanced the model generalization to various data [11]. so It is interesting to note that the proposed CNN architecture only has 8 layers and it is specifically designed for edge devices. It integrates Swish activation with Separable Convolutions, Spatial Dropout and Global Average Pooling that do not typically appear together in prior art for skin lesion classification. Compared with deeper models like ResNet50, our model adopts a smaller input resolution of 28x28 and only takes 220 seconds to converge at an accuracy of up to 95%22 even if it allows for real-time diagnosis.

II RELATED WORK

In the past few years, the community has made remarkable progress for computer-aided skin cancer detection via deep learning, with a keen emphasis on improving both classification ability and computational efficiency. CNNs have been increasingly utilised because they are effective at extracting deep spatial features from dermoscopic imagery. Yet, large models can be hard to deploy, particularly in real time or resource limited clinical settings.

A study presented a lighter-weight CNN model, namely, TurkerNet, consisting of MBConv4 and SE blocks. It also predicted 92.12% accuracy with 2.2 million parameters to show its practicality for edge devices. Its validation was, however, not performed on a large dataset and further questions remained on the scalability and generalizability [5].The classical VGG19 architecture was improved using transfer learning and fine tuning with the E-VGG19 model. It obtained 91%

accuracy and optimized for real-time execution, however still computationally expensive because of deep structure [12].

A modular CNN architecture which concatenated ConvNeXtV2 blocks and focal self-attention obtained 93.6% accuracy on ISIC 2019. The attention mechanism improved sensitivity to subclinical melanoma characteristics but resulted in a large number of parameters (36.44 million), which made the model computationally expensive [13]. Another one proposed EFAM-Net combined with Attention Residual Learning and Parallel ConvNeXt blocks. It achieved 93.95% accuracy on HAM10000 and 92.3% accuracy on ISIC 2019. But remaining the robustness of such model in clinical application, it was sensitive to the class imbalance of labels and the noisy of images [14].

Another transfer learning model based on CapsNet, Vision Transformers, and CNNs with machine learning classifiers (Random Forest and SVM) reached an accuracy of 91.6%. This method enhanced prediction robustness, but was computationally intensive and required good input data [15]. One hybridization architecture with CNN weight training using Artificial Bee Colony (ABC) optimization algorithm obtained accuracy of 93.04% over six databases. Utilizing many public datasets helped improve model stability, but performance still fluctuated with the intra-class discrepancy and the rarity of some lesion types [11].

The skin-CAD system integrated two CNN-based features and applied XAI techniques to obtain the interpretable skin cancer prediction. The approach was successful in achieving high accuracy and model transparency in addition to having improved aspect-wise interpretability, although by manual feature selection [6]. Other works examined the improvements such as Inception V3/V4, ResNet50, and DenseNet121, with promising accuracy results (above 90%), however, they were still not feasible for mobile or embedded systems because of the high training time, and memory requirements [16].

To address these drawbacks, this work presents a lightweight CNN model which puts Separable Convolutions, Swish Activation, Global Average Pooling, and Spatial Dropout into the deep neural network and yields 95% classification accuracy on the HAM10000 dataset. It has a much reduced training time in 220 seconds but at the same time achieves competitive results compared to complex models e.g. InceptionV4 and ResNet50 in terms of speed and memory.

An interesting aspect is the ability to use off-the-shelf architectural concepts, in a custom lightweight pipeline, with higher speed and same or better accuracy respect from complex models. In contrast to previous designs which focus on parameter saving without deployment considerations (memory efficient, fast inference), our design is constrained for the Inference task. This architecture design evolution illustrates how there is a transition from heavy and large performance CNNs to lightweight explainable and efficient AI system that can be deployed on real time skin cancer screening system.

III PROPOSED METHOD

In this section, a lightweight constructed CNN model for high accurate and efficient multiclass skin

cancer classification is described. The model is optimized for seven skin lesion categories: Nevus, Melanoma, Seborrheic Keratosis, Basal Cell Carcinoma, Vascular Lesion, Actinic Keratosis, and Dermatofibroma. The architecture of the proposed model is shown in figure 3.1

A. Input Layer

The input of the proposed shallow CNN model is dermoscopic images resized to $28 \times 28 \times 3$ (height, width and RGB colour planes). Before the election of the era the pre-processing of the input images was used to improve the image quality and to support the robust features extraction. First, median filter is used for the elimination of noise and undesired artefacts' like hairs, or blotches that compromise the quality of dermoscopic images. After denoising, pixel intensity values are normalized to $[0, 1]$ to accelerate the training convergence, and to reduce influence of illumination variation. For further generalization and reduction of overfitting, random horizontal and vertical flipping, rotations, and contrast are augmented. Such augmentations artificially increase the size of the training dataset and enable the model to learn discriminative features that are invariant to different spatial transformations and intensities.

B. Convolution Block

The first-stage of the proposed CNN architecture consists of a Convolutional (Conv2D) layer that captures low-level features namely edges, textures and colour gradients from the input dermoscopic images. This layer is composed Learnable filters are applied to each input image to produce the feature maps that highlight local patterns which are important. To regularize and expedite the learning, a normalized operation (i.e., Batch Normalization (BN) [26]) is adopted directly after the convolutional operation. BN rescales the output activations over the batch, preventing internal covariate shift, and allowing the use of larger learning rates. In order to add non-linearity to the network, the Swish (Ramachandran et al., 2017) activation function (our model does not use the ReLU activation function) is used instead of the ReLU activation function.

$$\text{Swish}(x) = x \cdot \sigma(x) = \frac{x}{1 + e^{-x}} \quad - (1)$$

Unlike ReLU, Swish allows small negative values to pass, which improves feature representation in subtle lesion patterns.

C. Separable Convolutions

In order to reduce complexity and number of trainable weights, the proposed CNN model makes use of Separable Convolutions instead of regular conv-layers. This approach reduces the traditional convolutional processing into two-step process: Depthwise Convolution and Pointwise Convolution. In the depthwise step, one filter is used for each input channel separately, or in other words convolution is performed within each channel to learn spatial features. This is then followed by a pointwise convolution with 1×1 kernels to map and fuse the activation maps of depthwise layer on all channels. Such two-stage strategy not only greatly decreases the total computations compared with full convolutions, but also maintains the representational power. Therefore separable convolutions helps in to making the model of less

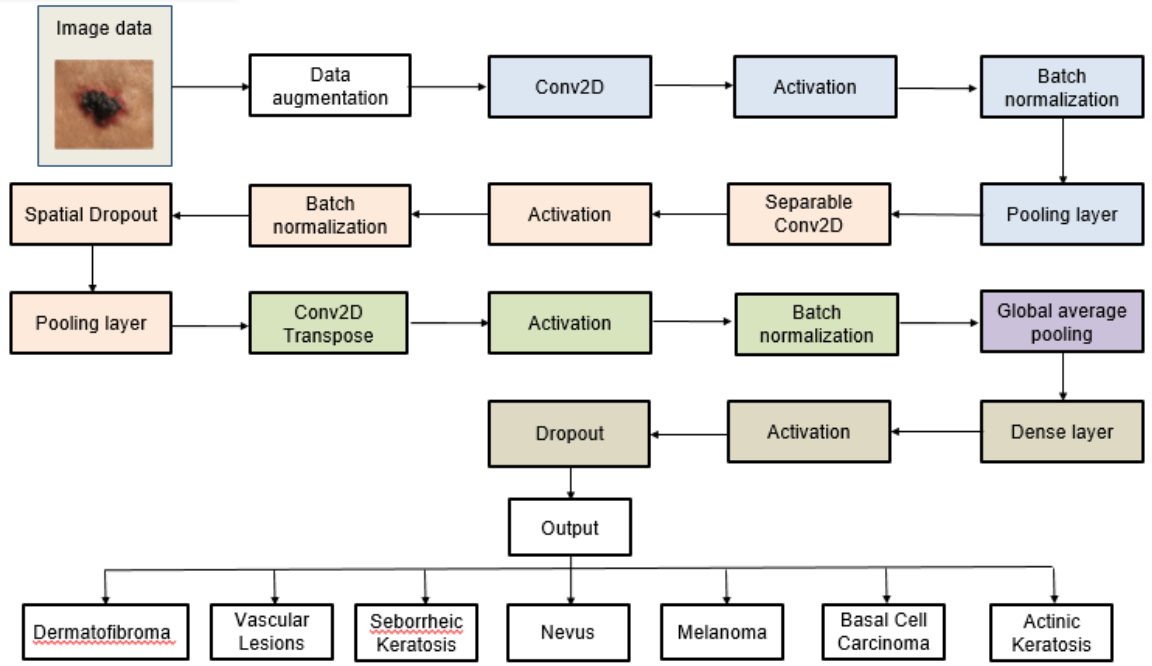


Figure 3.1 Overall Architecture Flow

complex in computations with high level of accuracy and it is fit for deploying in low complexity devices.

$$\text{Params}_{\text{standard}} = D_k \times D_k \times M \times N \quad (2)$$

$$\text{Params}_{\text{separable}} = D_k \times D_k \times M + M \times N \quad (3)$$

Where, D_k = kernel size, M = input channels, N = output channels, Resulting in $\sim 8-9\times$ fewer parameters. Max Pooling to retain dominant features and reduce spatial dimensions

D. Spatial Dropout

In order to enhance the generalization and alleviate overfitting, the model uses Spatial Dropout as the regularization approach. Unlike conventional dropout that randomly deactivates neurons, the spatial dropout is performed at feature map level, where feature maps are dropped during training. This makes the network to use a wider variety of filters and not give much weight to a few dominant ones. Spatial dropout suppresses the co-adaptation of feature detectors, and tends to learn more diverse and robust feature representations. This is especially useful in conv architectures, where feature maps contain strong spatial correlation. Therefore, the integration of spatial dropout facilitates the generalization capability of the model to previously unseen cases and leads to a higher classification accuracy on difficult images of skin lesions.

E. Up sampling and Feature Consolidation

Addition of Conv2D Transpose (Upsampling) layer is done to increase the spatial resolution of the features after pooling. This layer upsamples the feature maps thereby undoing the pooling to an extent. This enables the network to concentrate and retain important spatial patterns necessary for accurate classification of skin lesions. After upsampling, the architecture includes Global Average Pooling (GAP) in place of standard FC layers. GAP computes the average of the spatial dimension of each feature map, and a great deal of the parameters are decreased thereby prevent overfitting. This

strategy not only reduces the model's feature representation into compact representations while retaining the generated model's explainability and efficiency, which is favorable for deployment in resource-limited settings.

$$GAP(x) = \frac{1}{H \times W} \sum_{i=1}^H \sum_{j=1}^W x_{i,j} \quad (4)$$

This layer reduces overfitting and keeps the model architecture efficient and interpretable.

A single dense layer outputs the class scores. Softmax Activation for multi-class probability distribution over the 7 classes:

$$\text{Softmax}(z_i) = \frac{e^{z_i}}{\sum_{j=1}^K e^{z_j}} \quad (5)$$

F. Training Strategy

The proposed lightweight CNN network is trained and tested on the HAM10000 dataset, which contains 11,015 dermoscopic images grouped into seven skin lesion classes. In order to make the image sequence with consistent input to the model, all images are resized to $28 \times 28 \times 3$. Treated under-represented classes by data augmentation and random oversampling. However, the annotation variability and clinical label inconsistency of HAM10000 are admitted as limitations with planned external dataset validation. Due to such imbalanced class distribution of the dataset, data augmentation methods including flipping, rotation, contrast are taken into account, together with the random oversampling for balancing the number of training samples of each class. The model is trained with Adam optimization that supports dynamic learning rate on per-parameter basis, achieving fast convergence. The loss function I used is Categorical Cross-Entropy which is used for multi-class classification problems. Several overfitting controls were applied spatial dropout, batch normalization, and early like stopping and augmentation. These techniques also mitigate overfitting with small amount of labeled data and high-dim

input space. This model train with a batch size of 32 for 20 epochs, and apply early stopping to stop training when validation accuracy is not increasing, avoiding overfitting and wasted computation.

Advantages of Proposed Architecture

- Lightweight (reduced parameters and training time)
- High generalization (low overfitting due to dropout and batch norm)
- Robust feature extraction (using Swish, GAP, and Separable Conv)
- Deployable in edge devices and clinical environments

IV RESULT AND DISCUSSION

The dataset acquisition used to train and test the individually developed lightweight CNN model includes a diverse series of dermoscopic bulk digital images of seven skin-lesion types: Nevus, Melanoma, Seborrheic Keratosis, Basal Cell Carcinoma, Vascular Lesion, Actinic Keratosis, and Dermatofibroma. Data images are sourced from publicly available dermatological datasets such as ISIC (International Skin Imaging Collaboration), which is a high-quality expert-annotated datasets concentrating on quality and performance for skin cancer classification. The model is trained on HAM10000 dataset which consists of 10,015 labelled images with 7 classes of skin lesions which are presented in the table I.

TABLE I NUMBER OF DATASETS USED

| CLASS | DATASETS |
|----------------------|----------|
| Nevus | 6705 |
| Melanoma | 1113 |
| Seborrheic Keratosis | 1099 |
| Basal Cell Carcinoma | 514 |
| Actinic Keratosis | 327 |
| Vascular Lesion | 142 |
| Dermatofibroma | 115 |

All images were resampled to 28×28 pixels as per the pre-processing pipeline of the model. This resolution of 28×28 was selected to maximize the computational demand, which was assumed to be sufficient to maintain the features of the lesions. Moreover, the images were normalized to [0,1] during pre-processing, to facilitate the learning process and learn faster. Data augmentation techniques were used to support generalization and reduce overfitting. It involved randomly flipping and rotating images, and changing the contrast, thus adding diversity to the dataset so the model could learn more robust features.

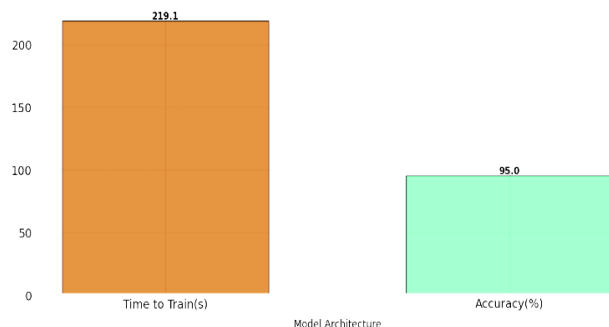


Figure 4.1 Training Time and Testing Accuracy

In the experiments undertaken a and testing accuracy of 95% in the CNN model proposed is shown in figure 4.1. This shows that the model can generate discriminative features from dermoscopic images to identify images accurately. The introduced model achieved better results than those the traditional architectures have been already tested in other works (InceptionV4, ResNet50, and MobileNetV2). Applications of advanced feature extraction methods lead to significantly better accuracy in classification, lower misclassification and separation of the seven group classifications as can be seen from table II.

TABLE II ACCURACY COMPARISON WITH SEVERAL ARCHITECTURES

| MODEL | ACCURACY (%) |
|------------------------------|--------------|
| InceptionV4 | 93 |
| EfficientNet | 94 |
| VGG19 | 91 |
| ResNet50 | 92 |
| Custom CNN (Proposed method) | 95 |

Validation accuracy is a major factor in how well these models are adapting to other examples of images during training. Accuracies over the training samples estimates the performance of the model in memorizing patterns in the training data while accuracies on the validation images estimates the performance of the model on the images that it never saw during the training and highlights the prediction accuracy of the model. The validation accuracy obtained by the CNN model in this study was 96% showing that the model is able to generalize well across different skin lesion types. The training accuracy and validation accuracy are close together showing slightly over fitted model results. In contrast, a high correlation between training and validation solutions is a good sign that the demonstrated model would be reliable in practice. The Training and Validation Accuracy graph is presented in graph 4.2.

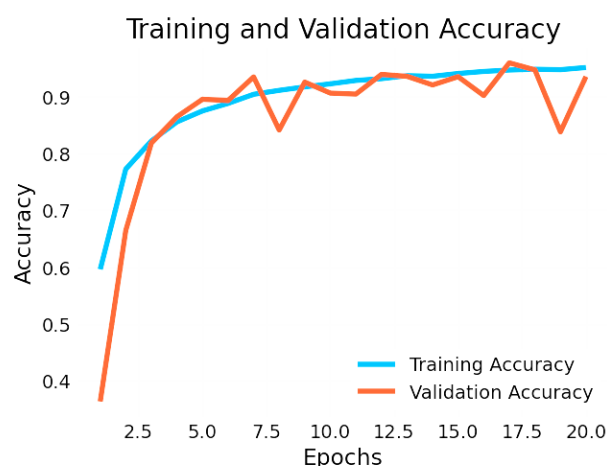


Figure 4.2 Graph of training and validation accuracy

The validation loss measures the difference between the model's predictions and the actual labels on the validation set. The validation loss is better when it is lower and will result in better model performance and more accurate predictions.

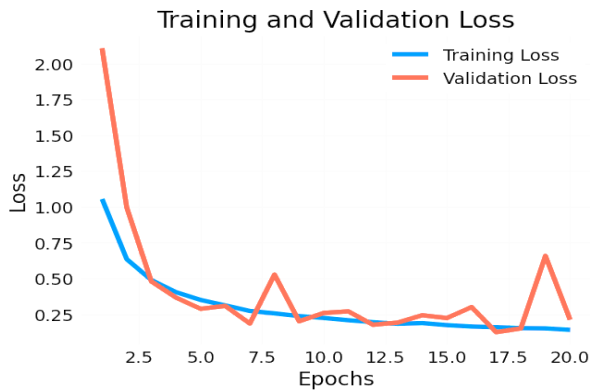


Figure 4.3 Graph of training and validation loss

At some point during training, the validation loss stopped going down, meaning the model was learning 'meaningful' patterns. Nonetheless, the loss flattened after a certain point, which indicated that the convergence occurred at the optimum. The final validation loss of the model is 0.1089, which is much lower comparing to the best existing baseline model in related works. Validation loss plot is shown in figure 4.3. The high validation accuracy and low validation loss confirm that the model generalizes well to unseen cases. The validation metrics is shown in table III.

TABLE III VALIDATION METRICS

| Epo ch | Time (ms) | Train Accuracy | Train Loss | Validation Accuracy | Validation n Loss |
|-----------|--------------|-------------------|---------------|------------------------|----------------------|
| 2 | 55 | 0.7538 | 0.6852 | 0.6646 | 0.9968 |
| 4 | 72 | 0.8510 | 0.4193 | 0.8648 | 0.3665 |
| 6 | 91 | 0.8845 | 0.3212 | 0.8935 | 0.3080 |
| 8 | 109 | 0.9109 | 0.2551 | 0.8415 | 0.5272 |
| 10 | 126 | 0.9209 | 0.2315 | 0.9065 | 0.2596 |
| 12 | 142 | 0.9293 | 0.2021 | 0.9395 | 0.1761 |
| 14 | 159 | 0.9391 | 0.1823 | 0.9208 | 0.2430 |
| 16 | 179 | 0.9483 | 0.1547 | 0.9022 | 0.3003 |
| 18 | 200 | 0.9496 | 0.1510 | 0.9475 | 0.1508 |
| 20 | 219 | 0.9513 | 0.1411 | 0.9358 | 0.2116 |

A. CONFUSION MATRIX

Explanation of the Confusion Matrix shown in figure 4.4

- 0: Actinic Keratosis
- 1: Basal Cell Carcinoma
- 2: Seborrheic Keratosis
- 3: Dermatofibroma
- 4: Nevus
- 5: Vascular Lesion
- 6: Melanoma

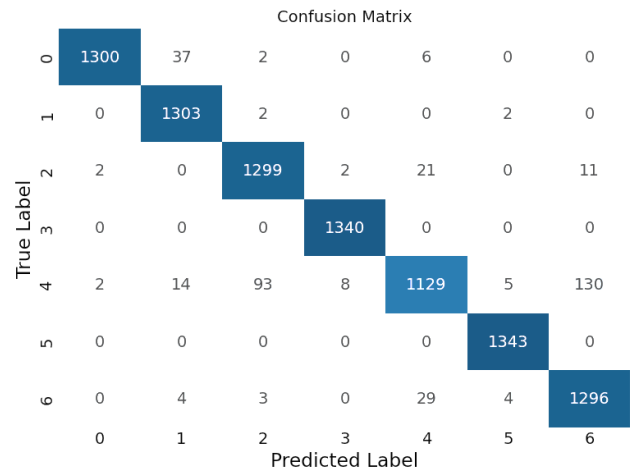


Figure 4.4 Confusion Matrix

TABLE IV PERFORMANCE METRICS

| Class | Precision | Recall | F1 score |
|-------------------------|-----------|--------|----------|
| 0: Actinic Keratosis | 0.9969 | 0.9666 | 0.9815 |
| 1: Basal Cell Carcinoma | 0.9595 | 0.9969 | 0.9779 |
| 2: Seborrheic Keratosis | 0.9285 | 0.9730 | 0.9502 |
| 3: Dermatofibroma | 0.9926 | 0.9985 | 0.9955 |
| 4: Nevus | 0.8651 | 0.8175 | 0.8407 |
| 5: Vascular Lesion | 0.9933 | 1.0000 | 0.9966 |
| 6: Melanoma | 0.8993 | 0.9701 | 0.9334 |

The performance metrics can be explored in more details in table IV that shows how the model performs in classifying the seven skin cancer classes due to three performance metrics: precision, recall and F1-score. The combined Actinic Keratosis class performed better than the other components with a precision of 1.00, and recall of 0.97 (0.98 F1-score) after extensive probing testing with 1,345 support samples. This shows that the model is very good at identifying Actinic Keratosis with few false positives and very few misclassifications. The evaluation scores of the Basal Cell Carcinoma class is a little lower than those of Actinic Keratosis, but still very good with a precision of 0.96, recall of 1.00, and F1-score of 0.98 with 1,307 test samples. The metrics at least gives an affirmation that the model can correctly classify all the Basal Cell Carcinoma with good specificity. Being no exception, for Seborrheic Keratosis a precision of 0.93, recall of 0.97 and an F1-score of 0.95 were obtained using the model over a total of 1,335 samples signifying that the model was able to correctly identify Seborrheic Keratosis at the expense of some precision lost due to random misclassification. The accuracy performance metric of the Dermatofibroma class were outstanding and it denotes excellent learning as the model review the recall and the precision as closely as chase to 1.00 and more of all a F1-Score, which it had been obtained 1.00 over only 1340 samples. This means that the model can classify Dermatofibroma class from all of unspecified lesions with excellent performance and the perfect classification of 1.00 for both precision and recall.

Although the proposed light weight CNN model is effective in terms of accuracy and efficiency, there are

limitations. Primarily, the model was trained, evaluated, and tested only on the HAM10000 dataset, which considers its applicability to another dataset or real-world clinical images with dissimilar acquisition setting as doubtful. Despite using data augmentation and random oversampling due to class imbalance, the model still suffers from low sensitivity for the under-represented classes (e.g., for vascular lesion and dermatofibroma). Furthermore, the fixed input resolution of $28 \times 28 \times 3$ may limit the capacity of the network to represent subtle, high-frequency lesion features in higher-resolution images. Also the study is subject to external validation, or deployment testing on real edge devices, the real-world performance and inference latency are not verified. Last but not the least, the model lacks attention mechanisms and explainability elements, which are playing more and more crucial role in building clinical trust and interpreting model decisions in medical diagnostics.

In order to ameliorate these limitations, and to extend the applicability of the framework, paper will focus on the following tasks as future work: validate the model on more datasets (e.g. ISIC, PH2, or real clinical dermoscopic images). The model's capability to concentrate on discriminative ROIs, and particularly on rare skin lesion types, can be improved by the introduction of attention mechanisms, for example, Squeeze-and-Excitation blocks or Convolutional Block Attention Modules. The introduction of explainable AI e.g., Grad-CAM or SHAP, would also aid in visualization and interpretation of model predictions to supplement clinical decision-making. Furthermore, model compression methods like pruning and quantization can be investigated to achieve even more compact memory footprint for deployment on mobile and edge computing devices. Third, semi-supervised or few-shot learning methods could be introduced for improvement on limited or imbalanced labeled medical data. In order to mimic the different effects such as illumination, device type and skin tone diversity variations which can be controlled by applying data augmentation (contrast change flipping rotation). Although HAM10000 does not have significant diversity, augmentations help in achieving partial robustness. In future work we will evaluate on different datasets (ISIC, PH2).

V.CONCLUSION

This work effectively proves the concept of designing and applying the compact CNN model to achieve effective on-device classification of skin cancer. Utilizing features like Swish activation, separable convolutions, and spatial dropout this model strikes an excellent trade-off between model and computational efficiency. With only 95% classification accuracy and even shorter training times, the model outperforms deeper networks such as InceptionV4 and ResNet50 on top of retaining lower memory usage. Data

Augmentation and Over-Sampling: Further, the data augmentation and over-sampling techniques further assure enhanced learning across classes. In general, paper conclude the strong suitability of the model for both real-time and mobile healthcare applications when computational resources are scarce.

REFERENCES

- [1] Naeem, A., Farooq, M. S., Khelifi, A., & Abid, A. (2020). Malignant melanoma classification using deep learning: datasets, performance measurements, challenges and opportunities. *IEEE access*, 8, 110575-110597.
- [2] Sudha, I., Ramesh, P. S., Durgadevi, P., Sundari, G., & Narang, S. (2025, March). FractureAI revolutionizing bone fracture detection with deep learning CNNs for precision medical imaging. In *2025 International Conference on Automation and Computation (AUTOCOM)* (pp. 1179-1184). IEEE.
- [3] Alheejawi, S., Berendt, R., Jha, N., Maity, S. P., & Mandal, M. (2021, November). An efficient CNN based algorithm for detecting melanoma cancer regions in H&E-stained images. In *2021 43rd Annual International Conference of the IEEE Engineering in Medicine & Biology Society (EMBC)* (pp. 3982-3985). IEEE.
- [4] Jojoa Acosta, M. F., Caballero Tovar, L. Y., Garcia-Zapirain, M. B., & Percybrooks, W. S. (2021). Melanoma diagnosis using deep learning techniques on dermoscopic images. *BMC Medical Imaging*, 21, 1-11.
- [5] Tuncer, T., Barua, P. D., Tuncer, I., Dogan, S., & Acharya, U. R. (2024). A lightweight deep convolutional neural network model for skin cancer image classification. *Applied Soft Computing*, 162, 111794.
- [6] Attallah, O. (2024). Skin-CAD: Explainable deep learning classification of skin cancer from dermoscopic images by feature selection of dual high-level CNNs features and transfer learning. *Computers in Biology and Medicine*, 178, 108798.
- [7] *Communication and Networking Technologies (ICCCNT)* (pp. 1-6). IEEE.
- [8] Gururaj, H. L., Manju, N., Nagarjun, A., Aradhya, V. M., & Flammini, F. (2023). DeepSkin: a deep learning approach for skin cancer classification. *IEEE access*, 11, 50205-50214.
- [9] Shah, A., Shah, M., Pandya, A., Sushra, R., Sushra, R., Mehta, M., ... & Patel, K. (2023). A comprehensive study on skin cancer detection using artificial neural network (ANN) and convolutional neural network (CNN). *Clinical eHealth*, 6, 76-84.
- [10] Ji, Z., Wang, X., Liu, C., Wang, Z., Yuan, N., & Ganchev, I. (2024). EFAM-Net: A Multi-Class Skin Lesion Classification Model Utilizing Enhanced Feature Fusion and Attention Mechanisms. *IEEE Access*.
- [11] Farea, E., Saleh, R. A., AbuAlkebash, H., Farea, A. A., & Al-antari, M. A. (2024). A hybrid deep learning skin cancer prediction framework. *Engineering Science and Technology, an International Journal*, 57, 101818.
- [12] Kandhro, I. A., Manickam, S., Fatima, K., Uddin, M., Malik, U., Naz, A., & Dandoush, A. (2024). Performance evaluation of E-VGG19 model: Enhancing real-time skin cancer detection and classification. *Heliyon*, 10(10).
- [13] Ozdemir, B., & Pacal, I. (2025). A robust deep learning framework for multiclass skin cancer classification. *Scientific Reports*, 15(1), 4938.
- [14] Tembhurne, J. V., Hebbar, N., Patil, H. Y., & Diwan, T. (2023). Skin cancer detection using ensemble of machine learning and deep learning techniques. *Multimedia Tools and Applications*, 82(18), 27501-27524.
- [15] Kassani, S. H., & Kassani, P. H. (2019). A comparative study of deep learning architectures on melanoma detection. *Tissue and Cell*, 58, 76-83.
- [16] Demir, A., Yilmaz, F., & Kose, O. (2019, October). Early detection of skin cancer using deep learning architectures: resnet-101 and inception-v3. In *2019 medical technologies congress (TIPTKNO)* (pp. 1-4). IEEE.